THE CLUSTER ORBITS WITH PERTURBATIONS OF KEPLERIAN ELEMENTS (COWPOKE) EQUATIONS

Chris Sabol
Craig McLaughlin
Kim Luu

20 March 2004

Final Report

AIR FORCE RESEARCH LABORATORY
Directed Energy Directorate
3550 Aberdeen Ave SE
AIR FORCE MATERIEL COMMAND
KIRTLAND AIR FORCE BASE, NM 87117-5776

STINFO COPY

Using Government drawings, specifications, or other data included in this document for any purpose other than Government procurement does not in any way obligate the U.S. Government. The fact that the Government formulated or supplied the drawings, specifications, or other data, does not license the holder or any other person or corporation; or convey any rights or permission to manufacture, use, or sell any patented invention that may relate to them.

This report has been reviewed by the Public Affairs Office and is releasable to the National Technical Information Service (NTIS). At NTIS, it will be available to the general public, including foreign nationals.

If you change your address, wish to be removed from this mailing list, or your organization no longer employs the addressee, please notify AFRL/DEBI, 3550 Aberdeen Ave SE, Kirtland AFB, NM 87117-5776.

Do not return copies of this report unless contractual obligations or notice on a specific document requires its return.

This report has been approved for publication.

//Signed//
VALERIE B. SKARUPA, GS-13
Project Manager

//Signed//
DAVID L. DINWIDDIE, DR-IV
Chief, Advanced Optics and Imaging Division

//Signed//
L. BRUCE SIMPSON, SES
Director, Directed Energy Directorate

REPORT DOCUMENTATION PAGE

Form Approved
OMB No. 0704-0188

1. REPORT DATE *(DD-MM-YYYY)*	**2. REPORT TYPE**	**3. DATES COVERED** *(From - To)*
20-03-2004	Final Report	4 Sep 02 – 30 Sep 03

4. TITLE AND SUBTITLE
The Cluster Orbits With Perturbations Of Keplerian Elements (COWPOKE) Equations

5a. CONTRACT NUMBER
In-House

5b. GRANT NUMBER
N/A

5c. PROGRAM ELEMENT NUMBER
63444F

6. AUTHOR(S)
Chris Sabol, Craig McLaughlin *, Kim Luu

5d. PROJECT NUMBER
5113

5e. TASK NUMBER
B3

5f. WORK UNIT NUMBER
AA

7. PERFORMING ORGANIZATION NAME(S) AND ADDRESS(ES)
AFRL/DEBI Det 15
535 Lipoa Parkway, Ste 200
Kihei, HI 96753

8. PERFORMING ORGANIZATION REPORT NUMBER
AFRL-DE-PS-TR-2004-1025

9. SPONSORING / MONITORING AGENCY NAME(S) AND ADDRESS(ES)
Air Force Office of Scientific Research

10. SPONSOR/MONITOR'S ACRONYM(S)

11. SPONSOR/MONITOR'S REPORT NUMBER(S)

12. DISTRIBUTION / AVAILABILITY STATEMENT
Approved for public release; distribution is unlimited.

13. SUPPLEMENTARY NOTES
*John D. Odegard School of Aerospace Sciences, Department of Space Sciences, 4149 Campus Rd, 530 Clifford Hall Grand Forks, ND 58202-9008

14. ABSTRACT
Recent developments have indicated that it is possible to express the relative equations of motion for space objects in non-circular orbits using mean Keplerian elements and low order expansions. This report provides the initial derivation of one such effort known as the Cluster Orbits With Perturbations Of Keplerian Elements (COWPOKE) equations. Given mean Keplerian elements and element differences, the COWPOKE equations describe spherical radial, cross-track, and along-track separations of the satellites as an explicit function of time. The framework of the equations allows for very high eccentricity reference orbits and for the inclusion of dynamic perturbations. Test cases using two-body dynamics show the utility of this approach.

15. SUBJECT TERMS
Relative motion, satellite formation flying, astrodynamics

16. SECURITY CLASSIFICATION OF:			**17. LIMITATION OF ABSTRACT**	**18. NUMBER OF PAGES**	**19a. NAME OF RESPONSIBLE PERSON**
a. REPORT UNCLASSIFIED	**b. ABSTRACT** UNCLASSIFIED	**c. THIS PAGE** UNCLASSIFIED	Unlimited	28	Chris Sabol
					19b. TELEPHONE NUMBER *(include area code)* 808-874-1594

Standard Form 298 (Rev. 8-98)
Prescribed by ANSI Std. 239.18

[This page intentionally left blank]

TABLE OF CONTENTS

FIGURES

ACKNOWLEDGMENTS

This research is sponsored by the Air Force Office of Scientific Research (AFOSR). The authors would like to thank Maj. William Hilbun of the Computational Mathematics Division and Dr. Clifford Rhoades of the Mathematics and Space Sciences Directorate of AFOSR for their support and commitment to basic research at the AMOS site. The authors would like to acknowledge the contributions of Dr. Chuck Matson, Mr. Paul Kervin, Lt. Col. Jeff McCann, Ms. Valerie Skarupa, Capt. Dale White, Cecilia Luna, Irma Aragon, and Dr. Joseph Janni in building and maintaining the AMOS basic research program. Finally, we would like to thank Rich Burns, now with the NASA Goddard Space Flight Center, for his previous contributions to AFRL formation flying efforts and Terry Alfriend of Texas A&M University for his useful comments over the last several years.

INTRODUCTION

Cluster orbits are defined as the relative trajectories of objects traveling through space in close proximity to each other. Clusters occur when satellites in similar orbits approach each other, groups of satellites fly in formation to perform specific mission functions, or several objects are launched or deployed from the same object. Each case has its own unique nuances, but the dynamics of how the objects move relative to each other are functionally the same.

The number of satellites in the geosynchronous belt has been steadily increasing for almost 40 years. While the number of satellites has been increasing, the space in the geosynchronous belt has not. This has led to more clusters of satellites operating in close proximity of each other and often unintentionally passing within kilometers of their neighbors[1]. Clusters of objects at this great altitude have been a long-standing challenge to space surveillance where the satellites can be mistaken for each other.

In recent years, there has been increasing interest in the use of satellites flying in formation. Several missions and mission statements have identified formation flying as a means of reducing cost and adding flexibility to space based programs or to accomplish goals that are not possible or very difficult to accomplish with a single satellite. These missions include NASA's Earth Observing-1 flying in formation with Landsat-7 and several European missions. In addition NASA has developed over 20 concepts for future missions involving formation flying. Many of these missions involve highly eccentric orbits.

During ballistic missile launches, several objects can achieve low earth orbit including the reentry vehicle, booster, fairings, and the possibility of several balloon-like decoys attempting to confuse missile defense systems. It is the responsibility of the missile defense system to track the cluster of objects and quickly identify the reentry vehicle.

The Cluster Orbits with Perturbations of Keplerian Elements (COWPOKE) equations can provide the theoretical foundation for analysis tools supporting a variety of applications. Optical space surveillance often reveals multiple satellites in a single telescope field of view. An understanding of the relative dynamics may allow for satellite identification based solely on relative position. Further research may apply these results to relative orbit determination of objects in a cluster or during close approach encounters. This approach may prove to be more accurate than performing orbit determination on the individual objects and determining differences. The equations might also be used to support the missile tracking experiments. If tracking sensors have limited fields of view, they may be required to track ballistic clusters individually; meaningful relative equations of motion may simplify the transition from object to object. Even if objects are tracked simultaneously, the relative equations of motion can be used as part of the discrimination process to identify balloon-like decoys. The COWPOKE equations would also be extremely relevant to satellite formation flying work, such as the initial Air Force Research Laboratory's TechSat 21 program, for formation flying design, analysis, and guidance and control applications. While a great deal of work has already been completed in support of formation flying missions, none provide the level of intuition and understanding as one that uses Keplerian elements. In addition, none of the work is accurate for long-term relative motion for orbits with eccentricities up to 0.7.

A simple set of equations describing the relative motion of spacecraft clusters is needed for analysis, design, and/or tracking of clusters. Much of the previous work in this field has relied on using Hill's equations[2] (also known as the Clohessy-Wiltshire equations[3]). Hill's equations describe the relative motion of spacecraft using a spacecraft-

centered coordinate system. However, Hill's equations assume that the reference orbit is circular, the objects are close together, and there are no perturbations to simple two-body motion. Several researchers have pointed out the severe limitations inherit in these assumptions. To rectify this, Gim and Alfriend[4] used energy methods to develop a state transition matrix to describe relative motion in non-circular orbits under the influence of perturbations. While closed form analytic solutions in a transformed variable space are valuable for analysis, these approaches may be awkward for many applications since transformations are required to go from the canonical variable space to more traditional representations of satellite orbits such as Keplerian elements. Additionally, most working level engineers lack the background to implement this approach. Previous work by Garrison et al.[5] developed equations of motion for elliptical orbits in terms of the true anomaly instead of time. Also, these equations were developed with rendezvous in mind and are developed only to second order in eccentricity. In addition, Melton[6] developed a state transition matrix for relative motion in eccentric orbits that is time dependent. Melton relied on some of the same foundations that are used in this paper, but the development was only to second order in eccentricity and is not accurate for orbits of high eccentricity. Baoyin et al,[12] did similar work but assumed matching orbital periods; this work also provides physical insight into formation flying in near circular orbits. This paper develops physically meaningful equations of relative motion for space objects in non-circular orbits using Keplerian elements.

Previous work by the authors[7] led to the development of a set of equations that describe the first order effects of Earth oblateness on the relative motion of objects in circular orbits. In addition, they developed a simple set of equations to describe the effects of Earth oblateness for polar orbits. Then, they further developed the equations to describe the motion for all inclinations[8]. Finally, they examined the long-term evolution of the relative motion for circular orbits and presented an approach to describe relative motion of satellites in elliptical orbits without perturbations and assuming matching periods[9]. This last step provided the building blocks for the COWPOKE equations.

In the past, equations of relative motion such as Hill's equations were developed by differencing the quasi-inertial equations of motion and mapping those differences into the rotating coordinate system. The result was a set of equations that describe the relative differences between the satellites typically in terms of radial, cross-track, and along-track components. Rather than using the traditional algebraic approach, the COWPOKE equations are developed using a geometric approach. Here, the geometric properties and definitions of Keplerian orbital elements will be used directly to map orbital element differences into the radial, cross-track, and along-track relative motion. In addition to the increased intuitiveness of a geometric approach, by using Keplerian orbital elements and differences in those orbital elements, we can take advantage of existing perturbation model development and incorporate meaningful dynamics into the relative equations of motion much easier than with the algebraic approaches.

There are challenges to this approach. First and foremost, the geometric properties of Keplerian elements are a function of the true anomaly, which has non-uniform variation with time. Ideally, analytical solutions are expressed in terms of the mean anomaly, which does vary linearly with time (outside the influence of perturbations). The relationship between the mean anomaly and eccentric anomaly is given by the well- known transcendental Kepler's equation. This research uses a series expansion to approximate the true anomaly as a function of time. A relation of this sort was successfully employed as part of the building blocks of the COWPOKE equations.

Using that one relationship, one can construct the relative motion of formation flying satellites by reconstructing the orbits individually based on their Keplerian elements and then differencing the two. This paper develops true equations of relative motion for clusters of objects. And, unlike the previous work, this research incorporates perturbation models and be generalized to account for small differences in semimajor axis. This results in a set of equations that describe the radial, cross-track, and along-track differences between two space objects in formation or a cluster based on Keplerian orbital element differences.

METHODS, ASSUMPTIONS, AND PROCEDURES

The formulation of the COWPOKE equations has three major challenges. The first is choosing a suitable reference frame for the relative equations of motion and expressing that frame in terms of Keplerian elements and element differences. The second is representing the geometrical true anomaly as a function of time. The final challenge is incorporating relevant perturbation effects. Only the first two challenges are addressed in this work.

Classical relative motion approaches use a Cartesian reference frame to describe relative motion. The components of this frame are radial, cross-track, and along-track differences. A limitation of this approach is that significant cross-mapping between components occurs when the separation distance between the satellites is not small. For instance, if two satellites travel together in a circular orbit but are separated by 0.01 rad in true anomaly, the relative position of one satellite with respect to the other will have an along-track separation as anticipated but will also have a radial component despite the fact that the satellites are at the same altitude and within the same orbit. Relative position difference components that are artifacts of the chosen coordinate frame, such as the one outlined in the preceding example, can greatly complicate the analysis of the relative motion.

A second coordinate frame choice is to use spherical separations. Here, the relative position difference is described by an altitude difference from a sphere having the radius of the reference satellite and angular components perpendicular to and along the reference satellite's direction of motion projected onto the sphere. These components, *dr*, *dxt*, and *dat*, are illustrated in Figure 1. The spherical reference frame is well-suited to describing the position of satellites in circular or near-circular orbits; however, when the orbital eccentricity becomes large, the spherical reference frame suffers from the same limitations as the Cartesian system.

A third option to describe the relative motion of satellites in elliptic orbits is to use an ellipsoidal reference system. This is similar to the spherical system except that the components are mapped along an ellipsoid rather than a sphere. This method has geometric challenges describing altitude variations and can still result in difficult to understand position differences.

For this formulation, we chose the spherical reference frame since it's slightly better than Cartesian for describing the orbital motion and provides the physical insight we desire. Additionally, it is a simple geometric mapping between spherical and Cartesian given the quantities described in this work if Cartesian coordinates are desired. In fact, the desired reference frame will likely be a function of application, but it is hoped that enough information is provided here so these equations can be easily reformulated in other reference frames.

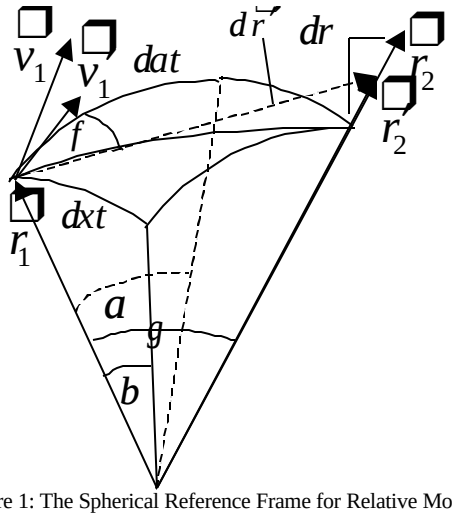

Figure 1: The Spherical Reference Frame for Relative Motion

The spherical coordinate system used here can be realized using position and velocity vectors of the two satellites:

$$\cos(\gamma) = \frac{\vec{r}_1 \bullet \vec{r}_2}{r_1 r_2}$$

$$r_2' = \frac{r_1}{\cos(\gamma)}$$

$$\vec{r}_2' = \left(\frac{\vec{r}_2}{r_2}\right) r_2'$$

$$d\vec{r}' = \vec{r}_2' - \vec{r}_1$$

$$\vec{v}_1' = \vec{v}_1 - \left(\frac{\vec{v}_1 \bullet \vec{r}_1}{r_1}\right)\vec{r}_1$$

$$\cos(\phi) = \frac{d\vec{r}' \bullet \vec{v}_1'}{dr' v_1'}$$

$$\sin(\beta) = \sin(\gamma)\sin(\phi)$$

$$\cos(\alpha) = \frac{\cos(\gamma)}{\cos(\beta)}$$

$$\begin{aligned} dr &= r_2 - r_1 \\ dxt &= r_1 \beta \\ dat &= r_1 \alpha \end{aligned} \tag{1}$$

Here, the auxiliary vector quantities, denoted by primes, are introduced so right planar triangles can be used in the determination of desired angular values. The spherical components can be expressed in terms of Keplerian elements by using the following definitions[10]:

$$\vec{r} = \frac{a(1-e^2)}{1+e\cos(\phi)} \begin{bmatrix} \cos(\Omega)\cos(\omega+\phi) - \sin(\Omega)\sin(\omega+\phi)\cos(i) \\ \sin(\Omega)\cos(\omega+\phi) - \cos(\Omega)\sin(\omega+\phi)\cos(i) \\ \sin(\omega+\phi)\sin(i) \end{bmatrix} \tag{2}$$

$$\vec{v} = \frac{-m}{\sqrt{ma(1-e^2)}} \begin{bmatrix} \cos(\Omega)(\sin(\omega+\phi)+e\sin(\omega)) + \sin(\Omega)(\cos(\omega+\phi)+e\cos(\omega))\cos(i) \\ \sin(\Omega)(\sin(\omega+\phi)+e\sin(\omega)) + \cos(\Omega)(\cos(\omega+\phi)+e\cos(\omega))\cos(i) \\ -(\cos(\omega+\phi)+e\cos(\omega))\sin(i) \end{bmatrix}$$

However, the resulting equations become difficult to manipulate. Instead, a simple geometrical mapping of Keplerian element and element differences into the spherical components of relative motion can be achieved with the following:

$$dr = \frac{(a_1+da)(1-(e_1+de)^2)}{1+(e_1+de)\cos(\phi_1+d\phi)} - \frac{a_1(1-e_1^2)}{1+e_1\cos(\phi_1)}$$

$$dxt/r_1 = \beta = -d\Omega\sin(i_1)\cos(\omega_1+d\omega+\phi_1+d\phi) + di\sin(\omega_1+d\omega+\phi_1+d\phi) \tag{3}$$

$$dat/r_1 = \alpha = (d\omega+d\phi)\cos(di) + d\Omega\cos(i_1)$$

The spherical cross-track and along-track terms are, in fact, approximations accurate to first order in the Keplerian elements differences. Figure 2 illustrates how these terms are derived.

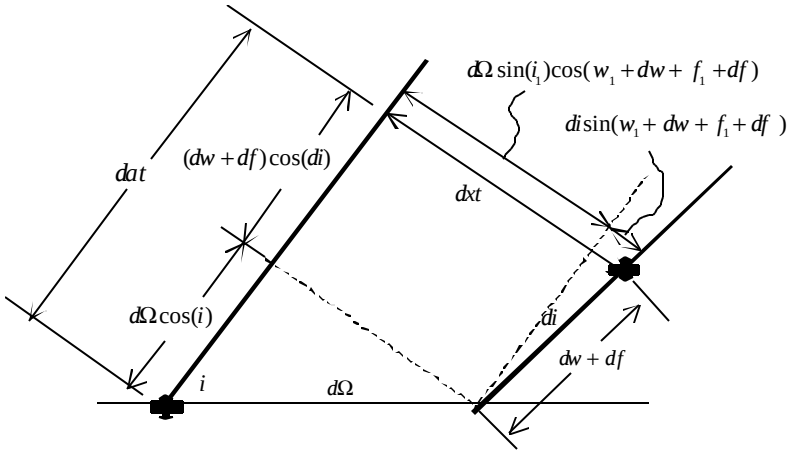

Figure 2: Spherical Components in Terms of Keplerian Elements and Element Differences

We can further simplify the radial expression to first order in the Keplerian element differences:

$$dr = \frac{1-e_1^2}{1+e_1\cos(f_1)}da + \frac{-a(2e_1+(1+e_1^2)\cos(f_1))}{(1+e_1\cos(f_1))^2}de + \frac{a_1e_1(1-e_1^2)\sin(f_1)}{(1+e_1\cos(f_1))^2}df \qquad (4)$$

From these Keplerian element representations of the relative motion, we can derive some physical insight into how orbital differences result in relative motion. If we assume a circular reference orbit, Eqs. (3) and (4) resemble the solutions to Hill's equations where the cross-track motion becomes a simple oscillation, the altitude difference maps directly into the radial motion with a periodic variation introduced by the eccentricity, and the altitude difference couples into the along-track component through the true anomaly resulting in a combination of secular and periodic effects[7].

While the equations above are useful and do help provide physical insight into the relative motion, they are expressed in terms of true anomaly. To express the relative motion as a function of time, one must express the above equations in terms of mean anomaly. At a fundamental level, this entails finding a suitable approximate solution to Kepler's equation. Battin provides several methods for doing so[10]. For the initial COWPOKE development, it was decided to use a Fourier-Bessel expansion of the true anomaly in terms of the mean anomaly and eccentricity.

Using the geometric properties of the true and eccentric anomalies and Kepler's equation, the following relationship can be found:

$$\frac{df}{dM} = \frac{\sqrt{1-e^2}}{(1-e\cos E)^2} \qquad (5)$$

This can be expressed in terms of a Fourier cosine series that introduces the Bessel functions, J_n:

$$\frac{df}{dM} = \sqrt{1-e^2}\left(B_0 + \sum_{k=1}^{\infty} B_k \cos(kM)\right),\ B_0 = \frac{1}{\sqrt{1-e^2}}\ , \tag{6}$$

$$B_k = \frac{2}{\sqrt{1-e^2}} \sum_{n=-\infty}^{\infty} \mathrm{J}_n(-ke)\, b^{|k+n|}\ ,$$

$$\mathrm{J}_n(-ke) = (-ke)^n \sum_{m=0}^{\infty} \frac{(-1)^m (-ke)^{2m}}{2^{2m+n}\, m!(n+m)!}\ ,$$

$$b = \frac{1-\sqrt{1-e^2}}{e},\ b^{|k+n|} = \left(\frac{e}{2}\right)^{|k+n|}\left[1 + \sum_{l=1}^{\infty}\left(\frac{e}{2}\right)^{2l} \frac{|k+n|}{l!} \prod_{j=1}^{l-1}\left(|k+n|+2l-j\right)\right]$$

Integrating this equation with respect to the mean anomaly provides an expression for the true anomaly in terms of the mean anomaly:

$$f = M + 2\sum_{k=1}^{\infty} \frac{1}{k}\left[\sum_{n=-\infty}^{\infty} \mathrm{J}_n(-ke)\, b^{|k+n|}\right] \sin(kM) \tag{7}$$

The result of this expansion is a sine series with coefficients that are power series in eccentricity. The lowest order of eccentricity for each coefficient series is k; thus the upper limit for k can be chosen based on the eccentricity of the reference orbit and the desired accuracy. Figure 3 plots eccentricity to the (k+1) power. The figure is meant to provide an indicator for the relative accuracy of Eq. (7) for a given eccentricity and choice of k. For instance, if one had a references eccentricity of 0.3 and desired series truncation errors below 1%, then one would choose to truncate the series at k=4 or the fourth power of eccentricity. When k=8, one sees errors below 10% up to e=0.7.

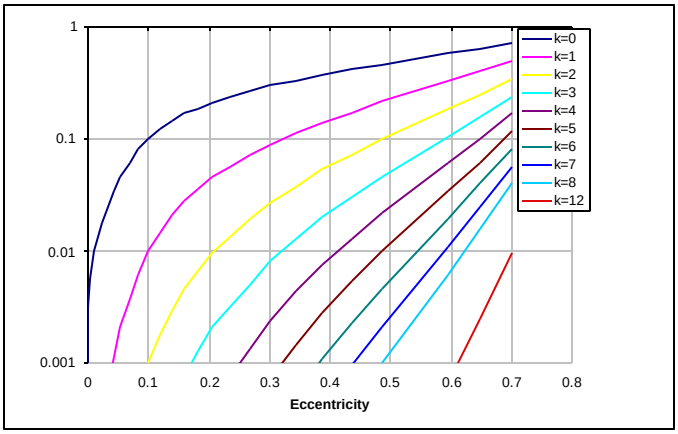

Figure 3: Relative Error Order of Magnitude for Eccentricity Series

Evaluating Eq. (7) up to the ninth frequency term (8M) yields:

$$f = M + \left(2e - \frac{1}{4}e^3 + \frac{5}{96}e^5 + \frac{107}{4608}e^7\right)\sin(M) + \left(\frac{5}{4}e^2 - \frac{11}{24}e^4 + \frac{17}{192}e^6 + \frac{43}{5760}e^8\right)\sin(2M) + \left(\frac{13}{12}e^3 - \frac{43}{64}e^5 + \frac{95}{512}e^7\right)\sin(3M) + \left(\frac{103}{96}e^4 - \frac{451}{480}e^6 + \frac{4123}{11520}e^8\right)\sin(4M) + \left(\frac{1097}{960}e^5 - \frac{5957}{4608}e^7\right)\sin(5M) + \left(\frac{1223}{960}e^6 - \frac{1987}{1120}e^8\right)\sin(6M) + \left(\frac{47273}{32256}e^7 - \frac{12412897}{5160960}e^9\right)\sin(7M) + \left(\frac{556403}{322560}e^8 - \frac{4745483}{1451520}e^{10}\right)\sin(8M) \quad (8)$$

In examining Eq. (8), one can see that the leading term in each of the eccentricity series does not decrease for all eccentricities; however, the second term in the eccentricity series is always negative and serves to reduce the magnitude of that frequency's contribution to the expansion as a whole. Thus, the amplitude of each frequency term decreases as the frequency increases allowing convergence of the entire expansion if enough terms are included in each individual eccentricity series. This means that for higher values of eccentricity, it is very important to include at least two or more terms for each eccentricity series. In Eq. (8), if the e^9 and e^{10} terms were left out of the 7*M* and 8*M* frequency terms, the error due to this truncation could be larger than if the 7*M* and 8*M* terms were not included at all. For higher values of eccentricity, care must be taken to make certain that enough terms are included in each eccentricity series to ensure one is not adding error with a given frequency term. The good news is that each eccentricity series converges fairly quickly so that powers of eccentricity at lower frequencies are much less important than at higher frequencies; this means that one can get away with fewer terms in each eccentricity series even if higher frequency terms are required. Additionally, for smaller values of eccentricity, 0.3 and below, truncation becomes much less of an issue since the e^2 factor greatly reduces the impact of the higher order terms in each eccentricity series and each higher frequency.

Truncation issues aside, the Fourier-Bessel series expansion of the true anomaly is an important component to the formulation of the COWPOKE equations; however, an additional step must be taken to map mean anomaly differences into true anomaly differences. This is accomplished by simply applying a first order perturbation to Eq. (8):

$$df = \frac{\partial f}{\partial M}dM + \frac{\partial f}{\partial e}de \quad (9)$$

The general formulation includes higher order element difference terms and coupling terms between the element differences but for cluster orbits, including the first order terms should provide accuracy to two orders of magnitude smaller than the separation distance. Including only the first order difference terms for the true anomaly expression yields:

$$
\begin{aligned}
df = &\left[1+\left(2e_1-\frac{1}{4}e_1^{\,3}+\frac{5}{96}e_1^{\,5}+\frac{107}{4608}e_1^{\,7}\right)\cos(M_1)+\right.\\
&2\left(\frac{5}{4}e_1^{\,2}-\frac{11}{24}e_1^{\,4}+\frac{17}{192}e_1^{\,6}+\frac{43}{5760}e_1^{\,8}\right)\cos(2M_1)+3\left(\frac{13}{12}e_1^{\,3}-\frac{43}{64}e_1^{\,5}+\frac{95}{512}e_1^{\,7}\right)\cos(3M_1)+\\
&4\left(\frac{103}{96}e_1^{\,4}-\frac{451}{480}e_1^{\,6}+\frac{4123}{11520}e_1^{\,8}\right)\cos(4M_1)+5\left(\frac{1097}{960}e_1^{\,5}-\frac{5957}{4608}e_1^{\,7}\right)\cos(5M_1)+\\
&6\left(\frac{1223}{960}e_1^{\,6}-\frac{1987}{1120}e_1^{\,8}\right)\cos(6M_1)+7\left(\frac{47273}{32256}e_1^{\,7}-\frac{12412897}{5160960}e_1^{\,9}\right)\cos(7M_1)+\\
&\left.8\left(\frac{63643}{35840}e_1^{\,8}-\frac{4745483}{1451520}e_1^{\,10}\right)\cos(8M_1)\right]dM+\left[\left(2-\frac{3}{4}e_1^{\,2}+\frac{25}{96}e_1^{\,4}+\frac{749}{4608}e_1^{\,6}\right)\sin(M_1)+\right.\\
&\left(\frac{5}{2}e_1-\frac{11}{6}e_1^{\,3}+\frac{17}{32}e_1^{\,5}+\frac{43}{720}e_1^{\,7}\right)\sin(2M_1)+\left(\frac{13}{4}e_1^{\,2}-\frac{215}{64}e_1^{\,4}+\frac{665}{512}e_1^{\,6}\right)\sin(3M_1)+\\
&\left(\frac{103}{24}e_1^{\,3}-\frac{451}{80}e_1^{\,5}+\frac{4123}{1440}e_1^{\,7}\right)\sin(4M_1)+\left(\frac{1097}{192}e_1^{\,4}-\frac{41699}{4608}e_1^{\,6}\right)\sin(5M_1)+\\
&\left(\frac{1223}{160}e_1^{\,5}-\frac{1987}{140}e_1^{\,7}\right)\sin(6M_1)+\left(\frac{47273}{4608}e_1^{\,6}-\frac{12412897}{573440}e_1^{\,8}\right)\sin(7M_1)+\\
&\left.\left(\frac{63643}{4480}e_1^{\,7}-\frac{4745483}{145152}e_1^{\,9}\right)\sin(8M_1)\right]de
\end{aligned}
\tag{10}
$$

The truncation issues for Eq. (10) are similar to those of Eq. (8) but are further compounded by the exponential factors produced when taking the partial derivative with respect to eccentricity. Note that the e^9 coefficient is twice as large as the e^7 coefficient in the $8M$ frequency series for the δe component.

For unperturbed satellite motion, we can express the mean anomaly as a function of time dM as a function of dM at epoch, semimajor axis difference, and time:

$$
M_1 = M_0+\left(\sqrt{\frac{m}{a_1^{\,3}}}\right)t,\; dM = dM_0+\left(\sqrt{\frac{m}{(a_1+da)^3}}-\sqrt{\frac{m}{a_1^{\,3}}}\right)t \tag{11}
$$

If one chooses, the mean motion terms in the above expression can be replaced by a second order perturbation of the mean motion with respect to da without significant error for most applications:

$$
dM = dM_0+\sqrt{m}\left(-\frac{3}{2}a_1^{-5/2}da+\frac{15}{8}a_1^{-7/2}da^2\right)t \tag{12}
$$

Eqs. (8), (10), and (11) can now be substituted into Eq. (3) to complete the COWPOKE equations for unperturbed satellite motion. Here are the COWPOKE equations with only first order eccentricity terms included in the expansion of the true anomaly and true anomaly difference:

$$dr = \frac{1-e_1^{\,2}}{1+e_1\cos(M_1+2e_1\sin(M_1))}da + \frac{-a(2e_1+(1+e_1^{\,2})\cos(M_1+2e_1\sin(M_1))}{(1+e_1\cos(M_1+2e_1\sin(M_1)))^2}de +$$
$$\frac{ae_1(1-e_1^{\,2})\sin(M_1+2e_1\sin(M_1))}{(1+e_1\cos(M_1+2e_1\sin(M_1)))^2}\left[(1+2e_1\cos(M_1))\left(dM_0+\left(\sqrt{\frac{m}{(a_1+da)^3}}-\sqrt{\frac{m}{a_1^{\,3}}}\right)t\right)\right]$$

$$\begin{aligned} dxt/r_1 = b = &-d\Omega\sin(i_1)\cos(w_1+dw+M_1+2e_1\sin(M_1)_1+ \\ &\left[(1+2e_1\cos(M_1))\left(dM_0+\left(\sqrt{\frac{m}{(a_1+da)^3}}-\sqrt{\frac{m}{a_1^{\,3}}}\right)t\right)\right])+ \\ &di\sin(w_1+dw+M_1+2e_1\sin(M_1)+ \\ &\left[(1+2e_1\cos(M_1))\left(dM_0+\left(\sqrt{\frac{m}{(a_1+da)^3}}-\sqrt{\frac{m}{a_1^{\,3}}}\right)t\right)\right]) \end{aligned} \tag{13}$$

$$dat/r_1 = a = \left(dw+\left[(1+2e_1\cos(M_1))\left(dM_0+\left(\sqrt{\frac{m}{(a_1+da)^3}}-\sqrt{\frac{m}{a_1^{\,3}}}\right)t\right)\right]\right)\cos(di)+d\Omega\cos(i_1)$$

Note that we have taken the linearized form of the radial component as presented in Eq. (4). From Figure 3, we would expect that these equations are accurate to the 1% level up to eccentricities of 0.1.

While this work does not currently include perturbations to the satellite dynamics, one of the key focuses of the COWPOKE development was to allow for the inclusion of additional force model effects. This can be accomplished by expressing the Keplerian elements and element differences as functions of time. This will be the focus of future work.

RESULTS AND DISCUSSION

Simulations were performed to quantify the error inherent in the approximations used in the COWPOKE formulation for two test cases. The first test case employed a near-circular, low-Earth orbit (e=0.01) and the second a high altitude eccentric orbit (e=0.7). The test cases were performed in the MATLAB environment using two-body dynamics; it is understood that that these simulations only measure the effectiveness of the COWPOKE equations to model two-body motion and are not indicative of the performance for real satellite motion.

Truth data for the simulations were determined by calculating the mean anomaly of each satellite as a function of time, converting the Keplerian elements to position and velocity vectors (with an algorithm taken from Vallado[11]), and then mapping the position differences into the spherical radial, cross-track, and along-track components described in Eq. (1). The COWPOKE results come from a direct mapping of the Keplerian element and element differences into those components using the methods described in the previous section. It should be noted that the angular cross-track and along-track values, a and b, were used for comparison purposes in the simulations rather than the arc-lengths, dxt and dat. Some additional error in the arc-lengths will be present due to the error in estimating the magnitude of the position vector of the reference satellite, but that is typically the same order of magnitude or smaller than the error in the angular separation.

Table 1 contains the orbital elements and element differences for the near-circular, low-Earth orbit (LEO) case; the reference satellite, satellite 1, has the initial Keplerian elements given in the "Reference Elements" column while the second satellite, satellite 2, has the initial Keplerian elements of the "Reference Elements" plus the "Element Differences." The simulation span covers 2 hours or just over one orbital period. The COWPOKE formulation includes only first order eccentricity terms and uses the radial component approximation; these equations were identical to Eq. (13).

Table 1: Keplerian Elements and Element Differences for LEO Test Case

	Reference Elements	Element Differences
a	7000 km	0.01 km
e	0.01	0.01
i	0.785 rad (45 deg)	0.01rad
Ω	0 rad (0 deg)	0.01 rad
ω	4.712 rad (270 deg)	0.01 rad
M_0	1.751 rad (90 deg)	0.01 rad

Figures 4-6 plot the spherical radial difference, angular cross-track, and angular along-track separations, respectively. Each figure actually contains two plots: the first shows the satellite separations described by the truth orbits and the COWPOKE approximation, and the second shows the differences between the truth and COWPOKE methods. Thus, the second plot in each figure is the error inherent in the given COWPOKE formulation.

Figure 4 shows the COWPOKE radial error to be around the 2% level. Figures 5 and 6 show the COWPOKE cross-track and along-track errors are below 1%. It is interesting to note that the radial and cross-track component errors have frequencies that appear to be once per orbit while the along-track component has an error frequency of twice per orbit. We test the COWPOKE approximations directly to determine the dominant sources of these errors.

Before continuing with the error analysis, it is useful to examine Figures 4-6 and observe the physical insight into the relative motion we can gain from the COWPOKE equations. Eq. (4) tells us that the relative motion in the radial direction is dominated by a once per orbit signature due to the eccentricity differences; the contributions from the semimajor axis difference are small, and the contribution from the true anomaly difference is an order of eccentricity smaller than the contribution from the eccentricity difference. Eq. (3) shows that the cross-track motion is comprised of once per orbit signatures from the inclination and right ascension of the ascending node differences. Eq. (13) indicates that the along-track motion is offset from zero due to the right ascension, argument of perigee, and mean anomaly differences but also has a once per orbit periodic signature with an amplitude of twice the reference eccentricity.

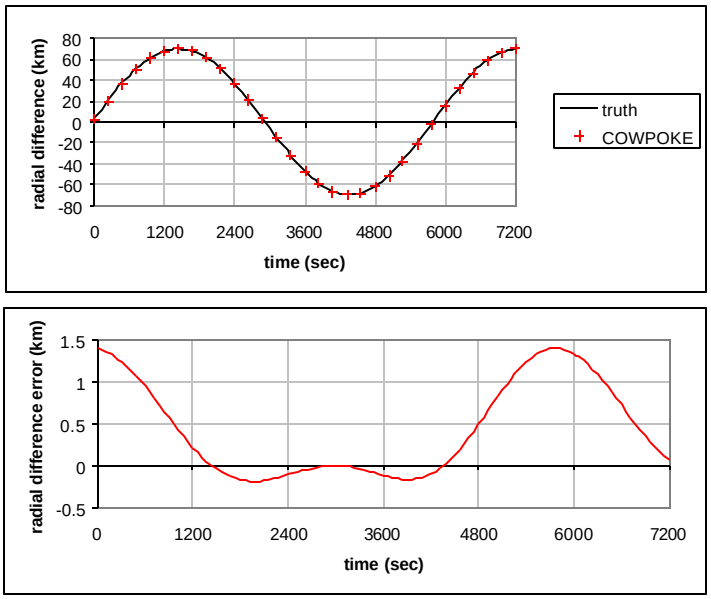

Figure 4: LEO Test Case Radial Differences and COWPOKE Errors

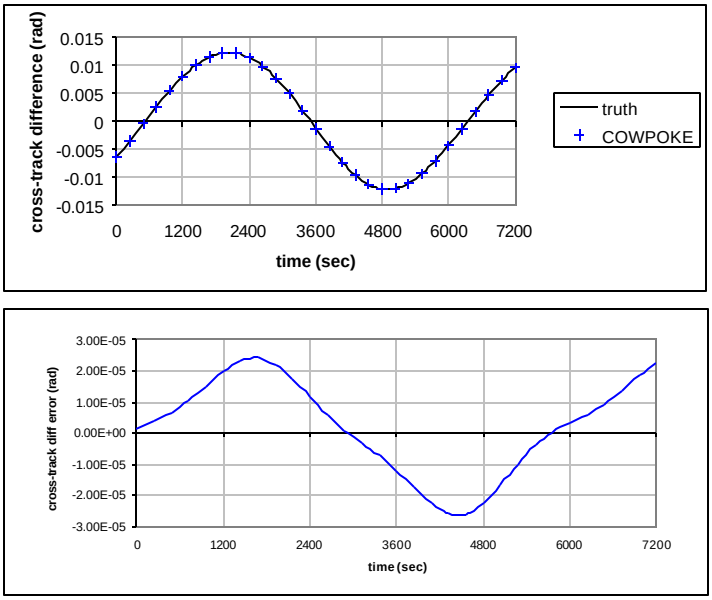

Figure 5: LEO Test Case Angular Cross-Track Differences and COWPOKE Errors

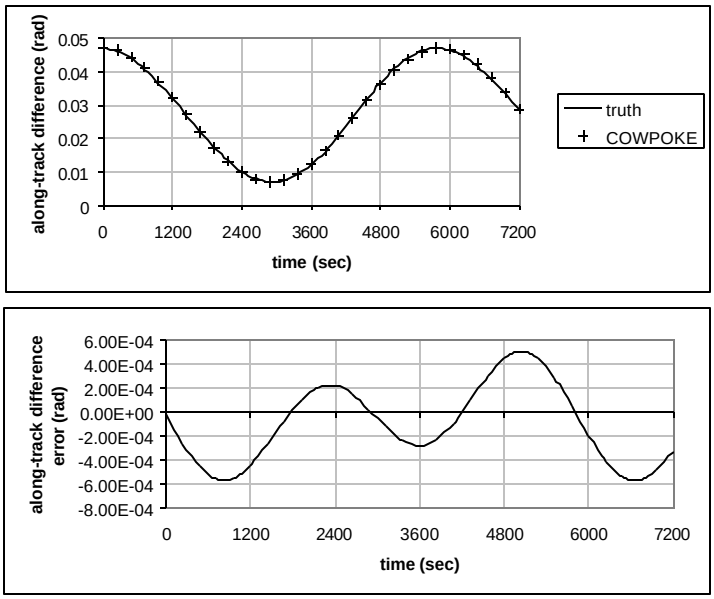

Figure 6: LEO Test Case Angular Along-Track Differences and COWPOKE Errors

Figure 7 plots the error in the first order Fourier-Bessel series expansion of the true anomaly of the reference satellite. From Figure 3, we expect to see around 1% error, and we do. Also note the twice per orbit signature in the error plot; this is also expected since the expansion only include once per orbit terms. Figure 8 plots the error in the approximation of the true anomaly difference; the error in this approximation is similar to the error in the true anomaly approximation. One sees that the dominant part of the along-track error is due to the COWPOKE approximation error of the true anomaly difference. If one chose, this error could be reduced by adding additional terms to the series approximation for this variable.

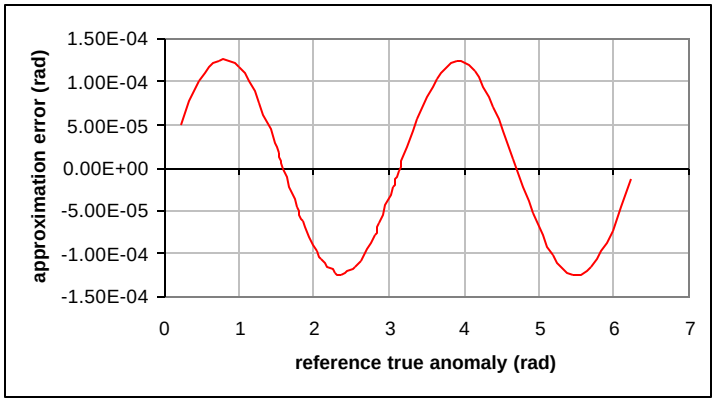

Figure 7: True Anomaly Approximation Error for LEO Test Case

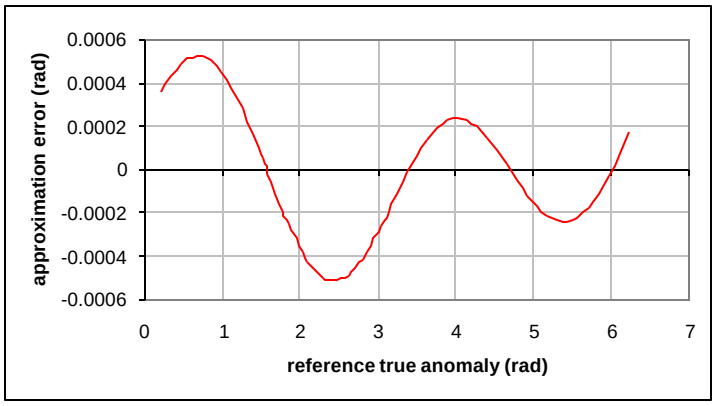

Figure 8: True Anomaly Difference Approximation Error for LEO Test Case

Figure 9 plots the errors in the COWPOKE coordinate system approximations for the LEO test case. One can see that the dominant part of the radial and cross-track errors is due to the coordinate system approximations made in the COWPOKE formulations. The radial component error can be reduced by using the analytical formulation for the radial difference while an improved description of the cross-track component would have to be derived to reduce the cross-track error.

Table 2 contains the orbital elements and element differences for the highly eccentric Earth orbit (HEO) test case. The simulation spans 12 hours or just over one orbital period. The COWPOKE formulation includes eighth order eccentricity up to frequency 6*M* and tenth order eccentricity in frequency 7*M* and 8*M*; these are all of the terms included in Eqs. (8) and (10). This test case does not use the radial component approximation.

Table 2: Keplerian Elements and Element Differences for HEO Test Case

	Reference Elements	Element Differences
a	27000 km	0.01 km
e	0.7	0.01
i	0.785 rad (45 deg)	0.01rad
Ω	0 rad (0 deg)	0.01 rad
ω	4.712 rad (270 deg)	0.01 rad
M_0	1.751 rad (90 deg)	0.01 rad

Figures 10-12 plot the spherical radial difference, angular cross-track, and angular along-track separations, respectively. As with Figures 4-6, the first plot in each figure shows the satellite separations described by the truth orbits and the COWPOKE approximation, and the second plot shows the differences between the truth and COWPOKE methods. Thus, the second plot in each figure is the error inherent in the given COWPOKE formulation for this highly eccentric test case.

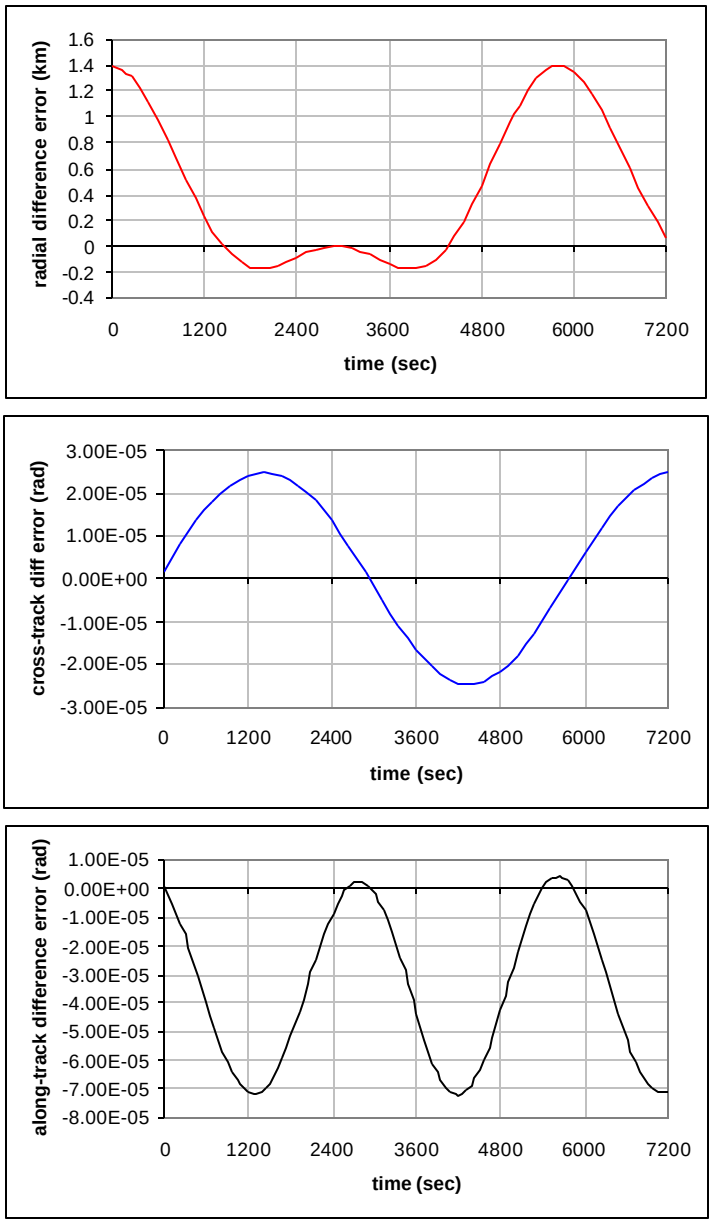

Figure 9: COWPOKE Coordinate System Approximation Errors for LEO Test Case

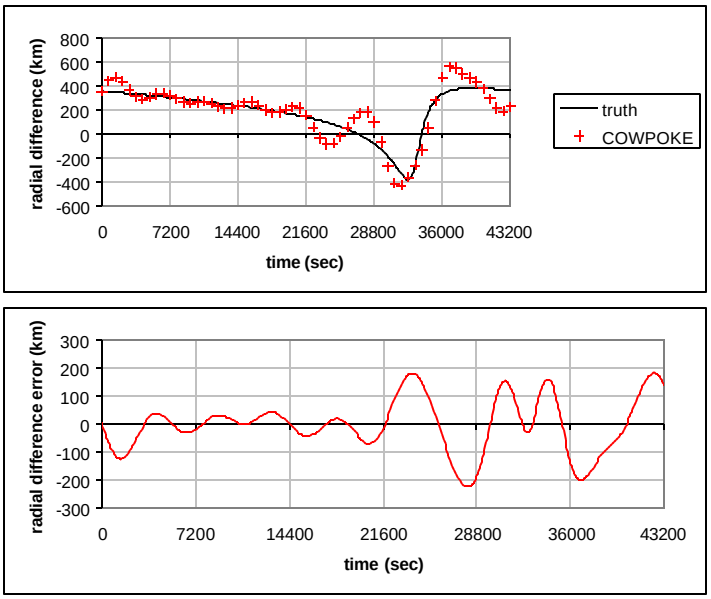

Figure 10: HEO Test Case Radial Differences and COWPOKE Errors

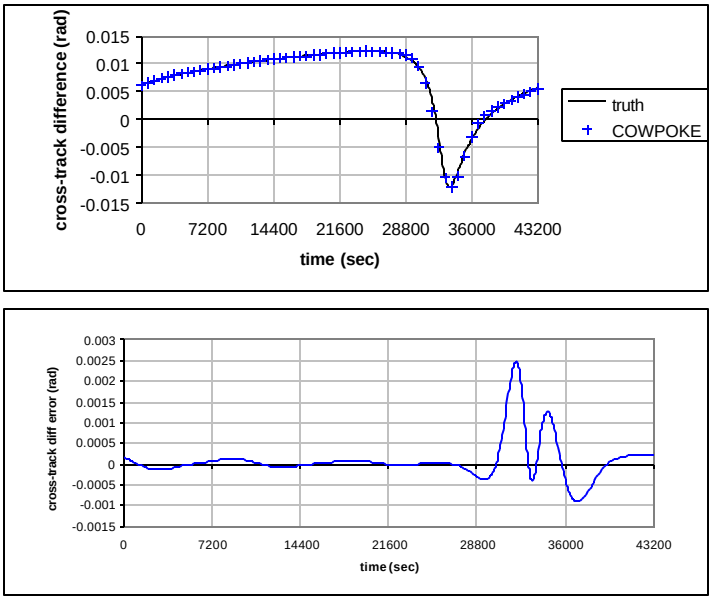

Figure 11: HEO Test Case Angular Cross-Track Differences and COWPOKE Errors

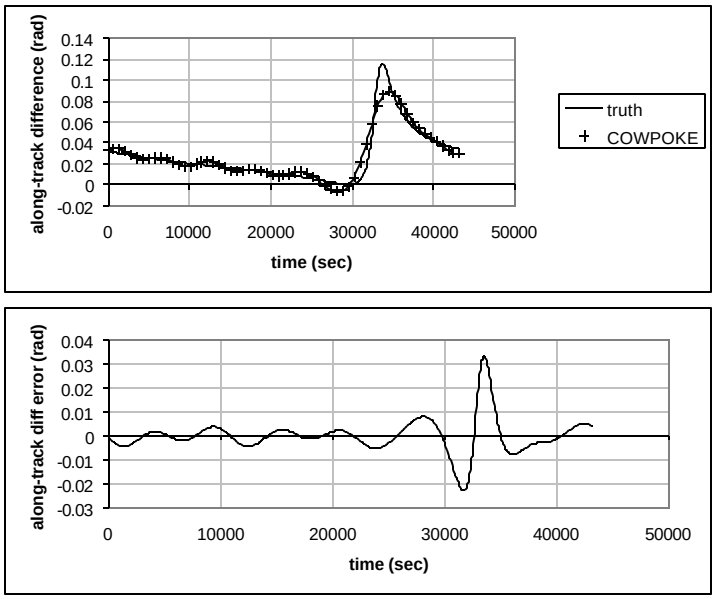

Figure 12: HEO Test Case Angular Along-Track Differences and COWPOKE Errors

Figure 10 shows the COWPOKE radial error to be significant with maximum errors being on the same order of magnitude as the relative altitude differences. Figures 11 and 12 show the COWPOKE cross-track and along-track errors are on the order of 10%. The sources of these errors can be determined by analyzing the approximations used in the COWPOKE formulation.

Figure 13 plots the error in the Fourier-Bessel series expansion of the true anomaly of the reference satellite. From Figure 3, we expect to see around 10% error, and we do along with a mixture of frequencies in the signature due to the series truncation. The error in the true anomaly approximation maps into the frequency terms and becomes the dominant source of error for the cross-track component. Figure 14 plots the error in the approximation of the true anomaly difference; the error in this approximation is an order of magnitude smaller than the error in the true anomaly approximation since we have removed an order of eccentricity in the differentiation process and replaced it by an eccentricity difference. Since the eccentricity difference is an order of magnitude smaller than the eccentricity, the eccentricity difference error is much smaller. One can see that the dominant part of the radial and along-track errors is due to the COWPOKE approximation error of the true anomaly difference and likely the eccentricity series truncation for the $8M$ frequency terms. If one chose, these errors could be reduced by adding higher order terms to the series approximations for these variables.

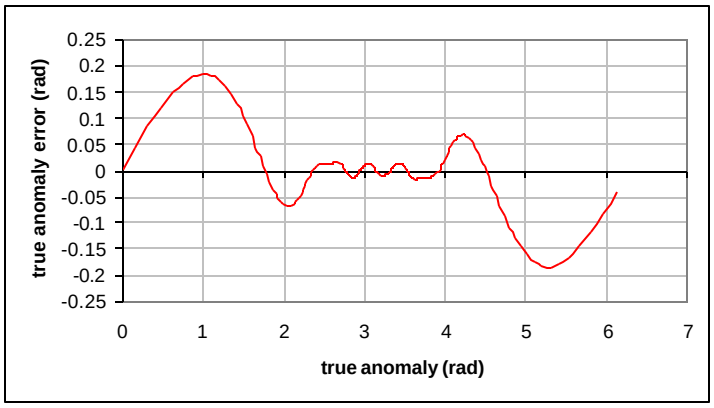

Figure 13: True Anomaly Approximation Error for HEO Test Case

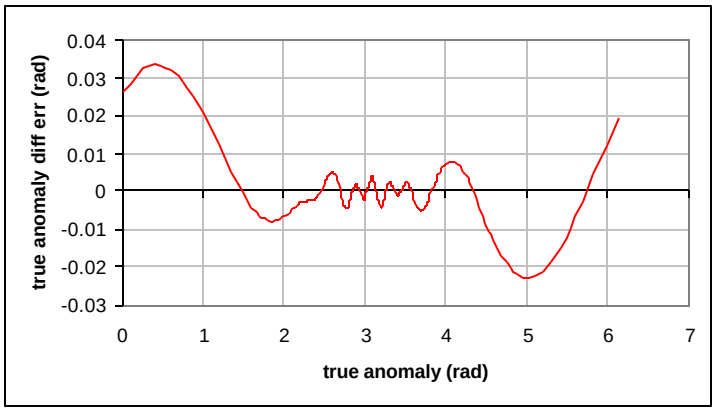

Figure 14: True Anomaly Difference Approximation Error for HEO Test Case

Figure 15 plots the errors in the COWPOKE coordinate system approximations for the HEO test case. There is no plot for the radial component since the radial approximation was not used, and thus the coordinate system error is zero. The cross-track and along-track components remain around or below the 1% level even for the high eccentricity case. It would seem that the coordinate system gives the COWPOKE equations an error bound of about 1%.

The cross-track and along-track errors for the HEO case are in line with expectations given the series truncations made in the COWPOKE formulation for this test case. The source of the radial error was larger than expected or desired. Further analysis of Eq. (4) shows that there is coupling between the true anomaly error and the eccentricity difference. The only way to mitigate this error is to reduce the error in the true anomaly difference approximation which can be accomplished by adding additional terms to the series expansion or by solving Kepler's equation iteratively. This would also serve to reduce the along-track errors as well.

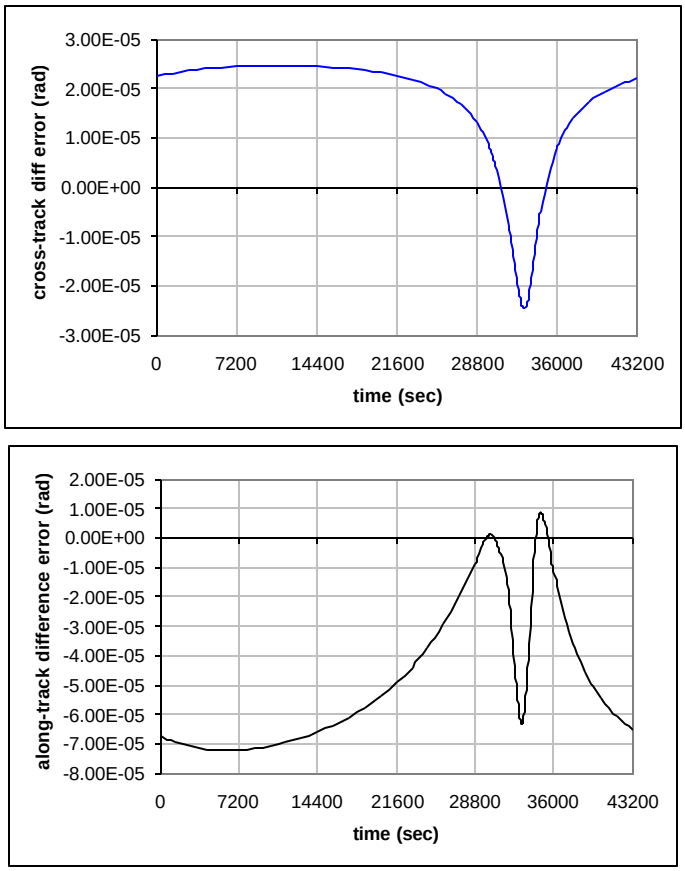

Figure 15: COWPOKE Coordinate System Approximation Errors for HEO Test Case

Despite the errors present in the HEO test case, the COWPOKE equations still model bulk of the relative motion fairly well, and the geometric foundation on which the equations are built can provide a fair amount of physical insight into the relative motion. For the HEO case, the physical insight is very similar to the LEO test case except we now observe that the true anomaly does not vary linearly with time. While the series expansions do not provide a great deal of insight into how the true anomaly varies, those who are familiar with the concept should be able to anticipate the trends. In Figures 10-12, we see that as the satellite moves towards apogee (recall the initial mean anomaly was 90 deg), the true anomaly rate slows which pushes the relative motion extrema to toward the time of perigee passage. It is interesting to note that initial true anomaly difference is a function of the mean anomaly difference, eccentricity, and the initial mean anomaly; a small mean anomaly difference at perigee of a highly eccentric orbit maps into a much larger true anomaly difference than if the initial conditions occurred at apogee. Additionally, one must be aware of this fact when considering error sources in the COWPOKE formulation since only first order differences in the Keplerian elements have been included in the equations above. Finally, from the COWPOKE equations, one can see that the argument of perigee also plays a significant role in the relative motion since the cross-track motion is dependent on both the true anomaly and the argument of perigee. The argument of perigee essentially controls the phasing between the cross-track and radial/along-track components of motion.

CONCLUSIONS

This paper derived the Cluster Orbits With Perturbations Of Keplerian Elements (COWPOKE) equations for unperturbed satellite motion. A general framework is provided to generate a set of equations which describe the relative motion between satellites in eccentric orbits explicitly as a function of the Keplerian elements of the reference satellite, Keplerian element differences, and time. This is accomplished using a geometric description of the separation between the satellites to form the basis of motion and then by using a Fourier-Bessel series expansion of the true anomaly in terms of the mean anomaly. True anomaly and radial differences are derived using first order perturbation methods. The resulting equations are meant to provide accurate representations of the relative motion between satellites, to be simple to implement, and to provide physical insight into the relative motion. Test cases show that this has been accomplished to a certain degree.

The geometric basis on which the COWPOKE equations are built is accurate to the 1% level when compared to the separation distances. This is currently the theoretical accuracy limitation. For most applications where the eccentricities are below 0.1, the COWPOKE equations are easily realizable and can be as accurate as the limitations of the geometric basis; however, the practical limitation for highly eccentric cases comes from generating enough terms in the series expansion of the true anomaly to reduce approximation errors to an acceptable level. This work shows that the radial component of the relative motion in our spherical reference system is particularly sensitive to true anomaly errors for high eccentricity orbits.

RECOMMENDATIONS

The next step in the development of the COWPOKE equations will be to include dynamic perturbation effects into the relative motion. Reference 8 has shown how secular effects due to Earth's oblateness can be incorporated using Keplerian elements and element differences. Simulations will also be performed to determine what other perturbations are required to support applications such as modeling geosynchronous clusters. We will also look into the invertibility of the COWPOKE equations. Here we will attempt to solve for Keplerian element differences based on desired or observed relative motion. This would be tremendously useful for formation design and geosynchronous close approach calculations.

REFERENCES

1. Abbot, R., R. Clouser, E. Evans, J. Sharma, "Close Geostationary Satellite Encounter Analysis: 1997-2001," presented at the AAS/AIAA Space Flight Mechanics Meeting, San Antonio, TX, 27-30 January 2002, AAS 02-115.

2. Hill, G. W., "Researches in the Lunar Theory," *American Journal of Mathematics*, Vol. 1, No. 1, 1878, pp. 5-26.

3. Clohessy, W. H., R. S. Wiltshire, "Terminal Guidance System for Satellite Rendezvous," *Journal of the Aerospace Sciences*, September 1960, pp. 653-658

4. Gim, D., K. Alfriend, "The State Transition Matrix of Relative Motion for the Perturbed Non-Circular Reference Orbit," presented at the AAS/AIAA Space Flight Mechanics Meeting, Santa Barbara, CA, 11-15 February 2001, AAS 01-222.

5. Garrison, J. L., T. G. Gardner, P. Axelrad, "Relative Motion in Highly Elliptical Orbits," *Advances in the Astronautical Sciences*, Vol. 89, No. 1, 1998, pp. 148-155.

6. Melton, R. G., "Time-Explicit Representation of Relative Motion Between Elliptical Orbits," *Journal of Guidance, Control, and Dynamics*, Vol. 23, No. 4, July-August 2000, pp. 604-610.

7. Sabol, C., R. Burns, C. McLaughlin, "Satellite Formation Flying Design and Evolution," *Journal of Spacecraft and Rockets*, Vol. 38, No. 2, March-April 2001, pp. 270-278.

8. McLaughlin, C., R. Burns, C. Sabol, K. Luu, "Modeling Relative Position, Relative Velocity, and Range Rate for Formation Flying," presented at the AAS/AIAA Astrodynamics Conference, Quebec City, Canada, 30 July -2 August 2001, AAS 01-457.

9. Swank, A., C. McLaughlin, C. Sabol, R. Burns, "Long Duration Analysis of the J2-Model Equations of Relative Motion for Satellite Clusters," presented at the AAS/AIAA Space Flight Mechanics Meeting, San Antonio, TX, 27-30 January 2002, AAS 02-185.

10. Battin, R. H., *An Introduction to the Mathematics and Methods of Astrodynamics*, AIAA Education Series, 1987, AIAA, Washington DC.

11. Vallado, D. A., *Fundamentals of Astrodynamics and Applications*, McGraw-Hill, New York, 1997

12. Baoyin, H., L. Junfeng, G. Yunfeng, "Dynamical behaviors and relative trajectories of the spacecraft formation flying," *Aerospace Science and Technology*, Vol. 6, 2002, pp. 295-301

DISTRIBUTION LIST

DTIC/OCP 8725 John J. Kingman Rd, Suite 0944 Ft Belvoir, VA 22060-6218	1 cy
AFRL/VSIL Kirtland AFB, NM 87117-5776	2 cys
AFRL/VSIH Kirtland AFB, NM 87117-5776	1 cy
Official Record Copy AFRL/DEBI/Chris Sabol	1 cy

[This page intentionally left blank]